Latin American Applied Research 37:127-132 (2007)

FE APPROACH FOR THERMODYNAMICALLY CONSISTENT GRADIENT-DEPENDENT PLASTICITY

S.M. VRECH and G. ETSE

Center of Numerical and Computational Methods in Engineering
University of Tucuman, Muñecas 730, 4000 Tucuman, Argentina
getse@herrera.unt.edu.ar

***Abstract*— In this work a dual-mixed FE-formulation for thermodynamically consistent gradient-dependent plasticity is proposed which leads to a fixed point iterative schema. At the constitutive level, the gradient-based Drucker-Prager model for cohesive-frictional material by Vrech and Etse (2005) is considered, which was formulated in the framework of the thermodynamically consistent gradient plasticity theory by Svedberg (1999).**

The robustness and efficiency of the proposed numerical tools are verified by means of computational analysis of inhomogeneous, uniaxial compression and tensile tests. These numerical results also demonstrate the capability of the gradient-dependent plasticity formulation to regularize the post peak response behavior regarding the mesh density as well as the influence of the internal length on the width of the plastic strains band.

***Keywords*— Gradient-elastoplasticity, non-local constitutive model, internal length, dual-mixed method, FE implementation.**

I. INTRODUCTION

The computational simulation of crack and shear band formations in cohesive-frictional materials and metals was advocated by many different authors, see a.o. Nadai (1931), Thomas (1961), Hill (1962), Rudnicki and Rice (1975), and more recently, Sobh (1987), Perič (1990), Ottosen and Runesson (1991), Willam and Etse (1990), Sluys (1992), Rizzi *et al.* (1995), Etse and Willam (1999). From these investigations follow the strong shortcomings of the so-called "smeared-crack" criterium to objectively predict localized failure modes of materials. To solve this deficit, regularization strategies of the softening regime are required.

In this work the regularization approach that is applied to the constitutive equations is based on non-local considerations in terms of higher gradients of the deformation field. The gradient functions are evaluated in the vicinity of the material points to obtain a spatial average of the deformation field. This is accomplished by defining the gradient of a selection of thermodynamic variables.

One of the crucial points in gradient dependent constitutive materials is the FE formulation to obtain efficient and robust solutions at the global or structural level. In this work a *dual mixed* FE procedure for thermodynamically consistent gradient-dependent plasticity based on CST elements is presented. The procedure considers two uncoupled but sequenced iterative processes for the update of the displacement field and plastic multiplier.

The efficiency and potentials of the *dual mixed* FE integration procedure of gradient-dependent plasticity is evaluated. Then, the regularization capabilities of the FE solutions of gradient-dependent plasticity are highlighted for bias and unbiased discretizations of boundary value problems in which the localized failure condition is fulfilled.

II. GRADIENT-DEPENDENT ELASTOPLASTICITY

After reviewing the relevant thermodynamic and constitutive equations, the yield condition of the consistent Drucker-Prager gradient-based elastoplastic model is presented. Thereby, the non-local character is restricted to the internal plastic variables.

A. Thermodynamic framework

The constitutive equations are obtained from thermodynamic consistency concepts. Under consideration of small strain kinematics, the free energy density of a strain gradient elastoplastic continuum can be expressed in an additive form as

$$\rho\Psi(\boldsymbol{\varepsilon}^e, \kappa, \boldsymbol{\nabla}\kappa) = \rho\Psi^e(\boldsymbol{\varepsilon}^e) + \rho\Psi^{p,l}(\kappa) + \rho\Psi^{p,g}(\boldsymbol{\nabla}\kappa) \quad (1)$$

where ρ is the material density.

The elastic free energy density $\rho\Psi^e$ is defined in terms of the elastic strain tensor $\boldsymbol{\varepsilon}^e$. The local and gradient free energy density contributions due to inelastic strains $\Psi^{p,l}$ and $\Psi^{p,g}$, are expressed in terms of the scalar hardening/softening variable κ. We observe in Eq. (1) that the gradient effects are only restricted to hardening/softening behavior via the inclusion of $\boldsymbol{\nabla}\kappa$.

We adopt the following expression for the elastic free energy density

$$\rho\Psi^e(\boldsymbol{\varepsilon}^e) = \frac{1}{2}\boldsymbol{\varepsilon}^e : \boldsymbol{E}^e : \boldsymbol{\varepsilon}^e \tag{2}$$

with $\boldsymbol{E}^e$ the fourth order elastic operator. For the local and gradient energy density due to inelastic strains, we assume

$$\rho\Psi^{p,l} = \frac{1}{2}H\kappa^2 \quad , \quad \rho\Psi^{p,g} = \frac{1}{2}l^2\boldsymbol{\nabla}\kappa\cdot\boldsymbol{H}^g\cdot\boldsymbol{\nabla}\kappa \tag{3}$$

The parameter H and the tensor $\boldsymbol{H}^g$ in Eqs. (3) are the *local* hard/soft modulus and the second order tensor of *non-local gradient*, respectively. These state parameters are defined as

$$H = \rho\frac{\partial^2\Psi^{p,l}}{(\partial\kappa^2)} \quad , \quad \boldsymbol{H}^g = \rho\frac{1}{l^2}\frac{\partial^2\Psi^{p,g}}{\partial(\boldsymbol{\nabla}\kappa)\otimes\partial(\boldsymbol{\nabla}\kappa)} \tag{4}$$

with

$$\det(\boldsymbol{H}^g) \geq 0 \tag{5}$$

There are three possible interpretations for the characteristic length l in Eqs. (4), see Svedberg (1998):

- a convenient dimensional parameter which allows that both, H and $\boldsymbol{H}^g$, get the same dimension,
- a physical entity that defines the characteristic measure of the microstructure, and
- a parameter that brings numerical stabilization to the local constitutive theory.

From the Coleman's relations follow the constitutive equations

$$\boldsymbol{\sigma} = \rho\frac{\partial\Psi}{\partial\boldsymbol{\varepsilon}} \quad , \quad \boldsymbol{\sigma} = \boldsymbol{E}^e : \varepsilon^e \tag{6}$$

where $\boldsymbol{\sigma}$ is the stress tensor and $\boldsymbol{\varepsilon}$ the strain tensor. The dissipative stress within the continuum is defined as

$$K = K^l + K^g \tag{7}$$

being the *local* dissipative stress

$$K^l = -\rho\frac{\partial\Psi^{p,l}}{\partial\kappa} = -H\kappa \tag{8}$$

and the *non-local gradient* one

$$K^g = \boldsymbol{\nabla}\cdot\left(\rho\frac{\partial\Psi^{p,g}}{\partial(\boldsymbol{\nabla}\kappa)}\right) = l^2\boldsymbol{\nabla}\cdot(\boldsymbol{H}^g\cdot\boldsymbol{\nabla}\kappa) \tag{9}$$

On the boundary $\partial\Omega$, the dissipative stress due to the gradient in Eq. (9) turns

$$K^{(g,b)} = -\boldsymbol{m}\cdot\rho\frac{\partial\Psi^{p,g}}{\partial(\boldsymbol{\nabla}\kappa)} = -l^2\boldsymbol{m}\cdot\boldsymbol{H}^g\cdot\boldsymbol{\nabla}\kappa \tag{10}$$

with the (outward) normal $\boldsymbol{m}$ to $\partial\Omega$.

B. Constitutive equations

We consider a convex set B of plastically admissible states defined as $B = \{(\boldsymbol{\sigma}, K) \mid \Phi(\boldsymbol{\sigma}, K) \leq 0\}$ with the convex yield function $\Phi = \Phi(\boldsymbol{\sigma}, K)$, and a dissipative potential $\Phi^* = \Phi^*(\boldsymbol{\sigma}, K)$, which turns Φ in case of associated plasticity. The rate equations for the inelastic strains $\dot{\boldsymbol{\varepsilon}}^p$ and the scalar hard./soft. variable $\dot{\kappa}$, take the forms

$$\dot{\boldsymbol{\varepsilon}}^p = \dot{\lambda}\frac{\partial\Phi^*}{\partial\boldsymbol{\sigma}} \quad \text{and} \quad \dot{\kappa} = \dot{\lambda}\frac{\partial\Phi^*}{\partial K} \tag{11}$$

where $\dot{\lambda}$ is the rate of the plastic parameter o multiplier.

From the Prandtl-Reuss additive decomposition of the total strain rate tensor into the elastic and plastic components that characterized the flow theory of plasticity and considering Eqs. (6), (8), (9), (10) and (11) follow the constitutive equations, in rate form

$$\dot{\boldsymbol{\sigma}} = \dot{\boldsymbol{\sigma}}^e - \dot{\lambda}\boldsymbol{E}^e\frac{\partial\Phi^*}{\partial\boldsymbol{\sigma}} \quad \text{with} \quad \dot{\boldsymbol{\sigma}}^e = \boldsymbol{E}^e : \dot{\boldsymbol{\varepsilon}} \tag{12}$$

$$\dot{K}^l = -\dot{\lambda}H\frac{\partial\Phi^*}{\partial K} \tag{13}$$

$$K^g = -l^2\boldsymbol{\nabla}\cdot(\boldsymbol{H}^g\cdot\boldsymbol{\nabla}\dot{\lambda})(\frac{\partial\Phi^*}{\partial K}) \tag{14}$$

$$K^{(g,b)} = l^2\boldsymbol{m}\cdot\boldsymbol{H}^g\cdot\boldsymbol{\nabla}\dot{\lambda}(\frac{\partial\Phi^*}{\partial K}) \tag{15}$$

The Kuhn-Tucker conditions complete the rate formulation of thermodynamically consistent gradient-dependent plasticity which, similarly to the local plasticity theory, are defined by

$$\dot{\lambda} \geq 0 \quad , \quad \Phi(\boldsymbol{\sigma}, K) \leq 0 \quad , \quad \dot{\lambda}\Phi(\boldsymbol{\sigma}, K) = 0 \tag{16}$$

The above indicated equations and theory were used by Vrech and Etse (2005) to define the gradient-based general Drucker-Prager constitutive model for cohesive-frictional materials. This model includes an isotropic hard/soft law to predict pre and post peak non linear material behavior.

C. Incremental constitutive equations

The updated stresses $\boldsymbol{\sigma}_{n+1}$ and K_{n+1} are obtained by applying a extension of the *Closest-Point-Projection-Method*, where $\boldsymbol{E}^e$, H and $\boldsymbol{H}^g$ define the projection metric.

The integration of the evolution laws in Eq. (11), by means of the Backward Euler rule, gives

$$\begin{aligned} \Delta\boldsymbol{\varepsilon}^p &= \Delta\lambda\frac{\partial\Phi^*_{n+1}}{\partial\boldsymbol{\sigma}} \\ \Delta\kappa &= \Delta\lambda\frac{\partial\Phi^*_{n+1}}{\partial K} \end{aligned} \tag{17}$$

Introducing the concept of *elastic trial* strain $\boldsymbol{\varepsilon}^{e,tr}_{n+1}$

$$\boldsymbol{\varepsilon}^{e,tr}_{n+1} = \boldsymbol{\varepsilon}^e_n + \Delta\boldsymbol{\varepsilon} \quad , \quad \boldsymbol{\varepsilon}^e_n = \boldsymbol{\varepsilon}_n - \boldsymbol{\varepsilon}^p_n \tag{18}$$

we obtain the updated stress tensor from Eq. (6) as

$$\boldsymbol{\sigma}_{n+1} = \boldsymbol{E}^e : \varepsilon^e_{n+1} \quad , \quad \varepsilon^e_{n+1} = \varepsilon^{e,tr}_{n+1} - \Delta\varepsilon^p \tag{19}$$

From $\lambda_{n+1} = \lambda_n + \Delta\lambda$ and Eqs. (13) and (14), the updated dissipative stress becomes

$$K_{n+1} = K_n + H\Delta\lambda\frac{\partial\Phi^*}{\partial K} - l^2\boldsymbol{\nabla}\cdot[H^g\cdot\boldsymbol{\nabla}(\Delta\lambda)]\frac{\partial\Phi^*}{\partial K} \tag{20}$$

The constrained boundary value problem based on the plastic multiplier increment $\Delta\lambda$, for all x in the surface Ω, results in a non homogeneous differential equation

$$-l^2\nabla\cdot(\overline{\boldsymbol{H}}^g\cdot\nabla(\Delta\lambda)) + h\Delta\lambda = \Phi^{e,tr}_{n+1} - \Phi_{n+1} \tag{21}$$

where

$$h = \frac{\partial\Phi}{\partial\boldsymbol{\sigma}} : \boldsymbol{E}^e : \frac{\partial\Phi^*}{\partial\boldsymbol{\sigma}} + \overline{H} \tag{22}$$

with

$$\overline{H} = H\frac{\partial\Phi}{\partial K}\frac{\partial\Phi^*}{\partial K} \tag{23}$$

and

$$\bar{\boldsymbol{H}}^g = \boldsymbol{H}^g\frac{\partial\Phi^*}{\partial K} \tag{24}$$

For the particular case of gradient isotropy, we obtain

$$\bar{\boldsymbol{H}}^g = \bar{H}^g\boldsymbol{I} \tag{25}$$

with $\bar{H}^g$ a positive, nonzero scalar.

Introducing the relation $\overline{c} = H_1^g lc$, being $H_1^g > 0$ the largest principal value of $\boldsymbol{H}^g$ and $c > 0$ a non-dimensional scalar constant, the Eq. (15), for all x on the boundary $\partial\Omega$, becomes

$$\boldsymbol{m}\cdot\boldsymbol{H}^g\cdot\nabla(\Delta\lambda) = -\frac{c}{l}H_1^g\cdot\Delta\lambda \tag{26}$$

D. Dual mixed FE strategy

The aim of this algorithm is to describe the evolution of the localization zone at the FE level during the hard/soft process.

Most of the FE-algorithms for gradient-dependent plasticity formulations are based on the coupling between the two main variables of the discrete variational problem: displacement field and plastic multiplier. The present approach leads to solve the plastic multiplier increment in a *dual mixed method*, and the algorithm procedure is implemented in a FE-code.

In case of gradient plasticity the yield criterion is non-locally defined as

$$\Phi^{e,tr,g}_{n+1} = \Phi^{e,tr}_{n+1} + l^2\nabla\cdot(\overline{\boldsymbol{H}}^g\cdot\nabla(\Delta\lambda)) = 0 \tag{27}$$

This expression encompasses the local yield condition in Eq.(21).

As Eq. (27) depends on the second order spacial derivatives of $\Delta\lambda$, the set of Eqs. (21), (23) and (26) need to be solved iteratively.

Introducing the notation

$$\boldsymbol{g} = \boldsymbol{H}^g\cdot\boldsymbol{\nabla}(\triangle\lambda) \tag{28}$$

for the gradient field, the BVP in Eq. (21) is rephrased as

$$\begin{aligned} -l^2\boldsymbol{\nabla}\cdot\boldsymbol{g} + h\Delta\lambda &= \Phi^{e,tr} - \Phi \\ (\boldsymbol{H}^g)^{-1}\cdot\boldsymbol{g} - \boldsymbol{\nabla}(\Delta\lambda) &= \boldsymbol{0} \end{aligned} \tag{29}$$

being $\boldsymbol{H}^g$ positive definite.

The boundary conditions of Eq. (26) with the Kuhn-Tucker conditions

$$\Delta\lambda \geq 0 \quad , \quad \Phi \leq 0 \quad , \quad \Delta\lambda\Phi = 0 \tag{30}$$

can be rewritten as

$$\Delta\lambda = -\frac{l}{cH_1^g}\boldsymbol{m}\cdot\boldsymbol{g} \tag{31}$$

The variational form of Eqs. (29), including the function spaces $\Lambda = L_2(\Omega)$ and $G = [H(\Omega)]^M$ with the spacial dimension M, takes the form

$$-l^2\int_\Omega \Delta\lambda'\boldsymbol{\nabla}\cdot\boldsymbol{g}d\Omega + \int_\Omega h\Delta\lambda'\Delta\lambda d\Omega = \int_\Omega \Delta\lambda'(\Phi^{e,tr} - \Phi)d\Omega \tag{32}$$

$$\int_\Omega \boldsymbol{g}'\cdot(\boldsymbol{H}^g)^{-1}\cdot\boldsymbol{g}d\Omega + \frac{l}{cH_1{}^g}\int_{\partial\Omega}\boldsymbol{g}'\cdot\boldsymbol{m}\otimes\boldsymbol{m}\cdot\boldsymbol{g}d(\partial\Omega) + \int_\Omega\boldsymbol{\nabla}\boldsymbol{g}'\Delta\lambda d\Omega = 0 \tag{33}$$

For CST finite elements, $\Delta\lambda$ is chosen piecewise constant in each element and $\boldsymbol{g}$ piecewise linear. In matrix notation, the above conditions take the form

$$\lambda' = \widehat{\lambda}'_e \quad , \quad \boldsymbol{g}' = \boldsymbol{\phi}_e{}^T\widehat{\boldsymbol{g}}'_e \quad , \quad \nabla\cdot\boldsymbol{g}' = \boldsymbol{B}_e{}^T\widehat{\boldsymbol{g}}'_e \tag{34}$$

where $\widehat{\lambda}'_e$ is the constant value of $\Delta\lambda$, $\widehat{\boldsymbol{g}}'_e$ the vector of nodal values of $\boldsymbol{g}$, while $\boldsymbol{\phi}_e{}^T$ contains the linear form functions. Replacing Eq. (34) in (32) and (33) and considering the complementary Kuhn-Tucker conditions, we obtain the finite element set of equations

$$-l^2\boldsymbol{B}_e{}^T\widehat{\boldsymbol{g}}_e + h\Delta\widehat{\lambda}_e = \widehat{\Phi}^{e,tr}_e - \widehat{\Phi}_e \tag{35}$$

$$\Lambda_{e=1}^{NEL}[(\boldsymbol{M}_e + \frac{l}{c}\boldsymbol{M}_e{}^{(b)})\widehat{\boldsymbol{g}}_e + A_e\boldsymbol{B}_e\Delta\widehat{\lambda}_e] = 0 \tag{36}$$

$$\Delta\widehat{\lambda}_e \geq 0 \quad , \quad \widehat{\Phi}_e \leq 0 \quad , \quad \Delta\widehat{\lambda}_e\widehat{\Phi}_e = 0 \tag{37}$$

with e= $1, 2, 3...NEL$, and

$$\boldsymbol{M}_e = \int_{\Omega_e}\boldsymbol{\phi}_e(\boldsymbol{H}^g)^{-1}\boldsymbol{\phi}_e^T\mathrm{d}\Omega \tag{38}$$

$$\boldsymbol{M}_e{}^{(b)} = \frac{1}{H_1^g}\int_{\partial\Omega_e}\boldsymbol{\phi}_e\boldsymbol{m}(\boldsymbol{\phi}_e\boldsymbol{m})^T\mathrm{d}(\partial\Omega) \tag{39}$$

Combining Eqs. (35) and (36), results

$$\Lambda_{e=1}^{NEL}[(\boldsymbol{M}_e + \frac{l}{c}\boldsymbol{M}_e{}^{(b)} + l^2\boldsymbol{C}_e)\widehat{\boldsymbol{g}}_e - \widehat{\boldsymbol{f}}_e] = 0 \tag{40}$$

Table 1: Iterative scheme to find $\Delta\widehat{\lambda}_e^{k+1}$ and $\widehat{\boldsymbol{g}}_e^{k+1}$

1. Set $\widehat{\boldsymbol{g}}^0 = \mathbf{0}$
2. For a given $\widehat{\boldsymbol{g}}^{(k)}$, solve $\widehat{\boldsymbol{g}}_e^{(k)}$ as follows:
   $\widehat{\Phi}_e^{e,tr,g(k)} = \widehat{\Phi}_e^{trial} + l^2\boldsymbol{B}_e^e\widehat{\boldsymbol{g}}_e^{(k+1)}$
   If $\widehat{\Phi}_e^{e,tr,g(k)} > 0 \;\Rightarrow\; \Delta\widehat{\lambda}_e^{(k+1)} = \frac{1}{h}\widehat{\Phi}_e^{e,tr,g(k)}$
   and $\widehat{\Phi}_e^{(k+1)} = 0$
   If $\widehat{\Phi}_e^{e,tr,g(k)} \leq 0 \;\Rightarrow\; \Delta\widehat{\lambda}_e^{(k+1)} = 0$
   and $\widehat{\Phi}_e^{(k+1)} = \widehat{\Phi}_e^{e,tr,g(k)}$
3. Solve $\widehat{\boldsymbol{g}}^{k+1}$ from
   $\boldsymbol{f}^{(k+1)} = \Lambda_{e=1}^{NEL}\widehat{\boldsymbol{f}}_e^{(k+1)}$
   $(\boldsymbol{M} + \frac{l}{c}\boldsymbol{M}^{(b)} + l^2\boldsymbol{C})\widehat{\boldsymbol{g}}^{(k+1)} = \widehat{\boldsymbol{f}}^{(k)} \longrightarrow \widehat{\boldsymbol{g}}^{(k+1)}$
4. Check convergence
   If $|\widehat{\boldsymbol{g}}^{(k+1)} - \widehat{\boldsymbol{g}}^{k}| < tol$
   and $\frac{1}{NEL}\sum_{e=1}^{NEL}|\Delta\widehat{\lambda}_e^{(k+1)} - \Delta\widehat{\lambda}_e^{(k)}| < tol$, stop.
   Else go to 2 and continue iteration

where

$$\begin{aligned} \boldsymbol{C}_e &= \frac{V_e}{h}\boldsymbol{B}_e\boldsymbol{B}_e^T \\ \boldsymbol{f}_e &= -V_e\boldsymbol{B}_e\Delta\widehat{\lambda}_e^1 \\ \Delta\widehat{\lambda}_e^1 &= \frac{1}{h}(\widehat{\Phi}_e^{e,tr} - \widehat{\Phi}_e) \end{aligned} \tag{41}$$

being V_e the volume of the element.

Finally, the system of Eqs. (35) and (40) is reformulated as

$$h\Delta\widehat{\lambda}_e' = \widehat{\Phi}_e^{e,tr,g} - \widehat{\Phi}_e \tag{42}$$

$$(\boldsymbol{M} + \frac{l}{c}\boldsymbol{M}^{(b)} + l^2\boldsymbol{C})\widehat{\boldsymbol{g}} = \widehat{\boldsymbol{f}} \tag{43}$$

where

$$\widehat{\Phi}_e^{e,tr,g} = \widehat{\Phi}_e^{e,tr} + l^2\boldsymbol{B}_e^T\widehat{\boldsymbol{g}}_e \tag{44}$$

with the notation

$$\begin{aligned} \boldsymbol{M} = \Lambda_{e=1}^{NEL}\boldsymbol{M}_e \quad &, \quad \boldsymbol{M}^{(b)} = \Lambda_{e=1}^{NEL}\boldsymbol{M}_e^{(b)} \\ \boldsymbol{C} = \Lambda_{e=1}^{NEL}\boldsymbol{C}_e \quad &, \quad \widehat{\boldsymbol{f}} = \Lambda_{e=1}^{NEL}\widehat{\boldsymbol{f}}_e \end{aligned} \tag{45}$$

For the special case of *local* theory, $l = 0$ in Eq. (44) and $\widehat{\Phi}_e^{e,tr,g} = \widehat{\Phi}_e^{e,tr}$. Thus, $\widehat{\lambda}_e'$ can be obtained from Eqs. (42) and (37).

Provide $\widehat{\Phi}_e^{e,tr}$ is known, the problem defined by Eqs. (42), (43) and (37) is solved using the fixed point iterative scheme shown in Table 1.

III. NUMERICAL ANALYSIS

Numerical simulations were performed for a rectangular specimen under plane strain conditions. Due to the symmetry of the problem, only one quarter of the patch was considered in the FE analysis. Uniform vertical displacements were prescribed on the top edges as can be seen in Fig. 1-(a) for both, the compression and the tensile tests.

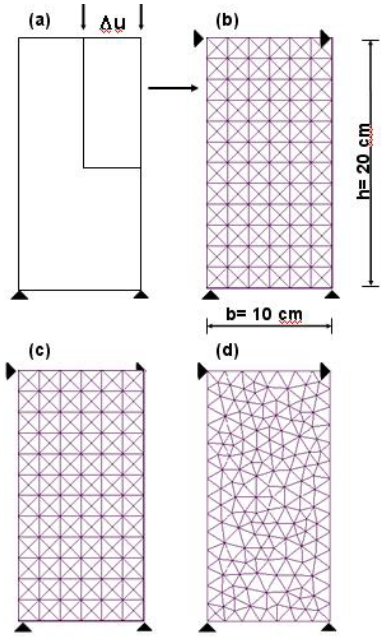

Figure 1: Uniaxial compression and tensile tests. Boundary condition and geometry discretizations.

In the FE analysis, bias and unbiased meshes in Figs. 1-(b) and 1-(c,d) were used. The properties of the non-linear Drucker-Prager material are

f_t'=1200 $\frac{kg}{cm^2}$ $\rho = \frac{f_c'}{f_t'} = 2$

E=2100000 $\frac{kg}{cm^2}$ ν= 0.3

$\overline{H}$= -150000 $\overline{H}_g$= 5000.

The typical response curves for compressive and tensile tests with both *local* and *non-local gradient* model materials, were plotted in Figs. 2 and 3 respectively. The softening behavior was evaluated at the residual force point.

In the compression test, different widths of the localization zone were obtained with the *local* and *non-local*

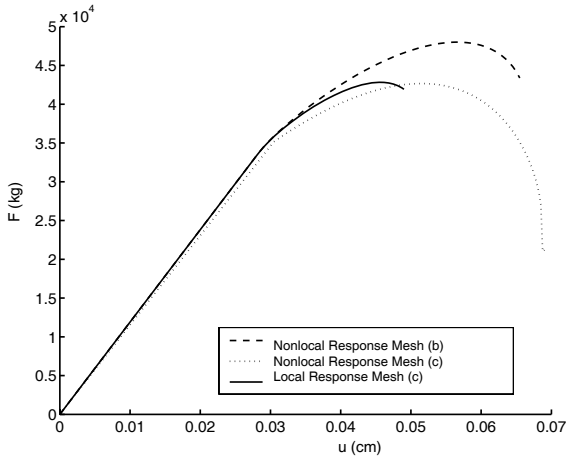

Figure 2: Force-displacement curves for compressive test with *local* and *non-local gradient* material models.

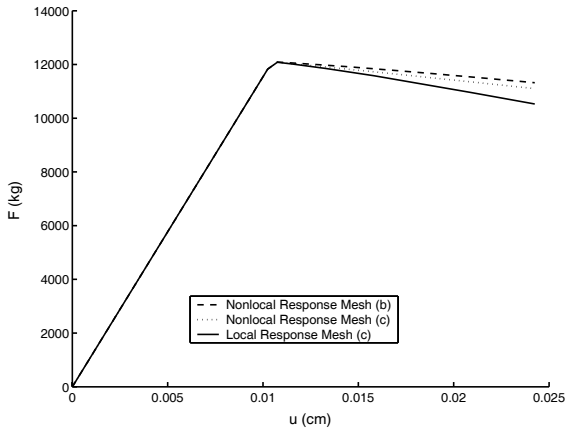

Figure 3: Force-displacement curves for tensile test with *local* and *non-local gradient* material models.

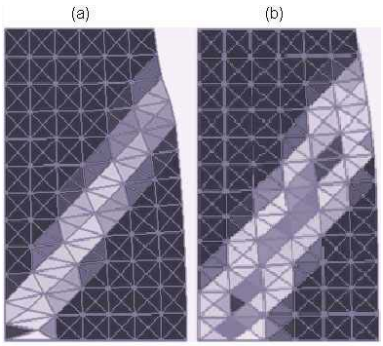

Figure 4: Response in compressive test for *local* (a) and *non-local gradient* (b) Drucker-Prager model with l= 2.5 cm.

Drucker-Prager material models. Using the bias mesh of Fig. 1-(b), for the local constitutive model the final width of the localization zone is fixed by the size of the typical element whereas for the non-local material, the internal length l= 2.5 cm defines the final width of the failure zone as can be observed in Fig. 4-(a) and (b), respectively.

Therefore, in *non-local gradient* Drucker-Prager material, the width of the plastic zone coincides with the internal length l.

In the tensile test, we analyze the predictions with the bias and the unbiased meshes in Fig. 1-(b) and 1-(c) respectively. The internal length l=3.5 cm was considered. The width of the plastic strain zone at final stage coincides with l. Figure 5 shows that the final width of the plastic strain zone is similar for both meshes. We conclude that bias and unbiased meshes lead to similar results when gradient-dependent materials are considered.

For the unbiased mesh in Fig. 1-(c), the FE analysis was performed with two different internal lengths: l= 2.5 cm and l= 5.0 cm. As before, we observe that the characteristic length l defines the width of the the plastic strain zone. These results are shown in Fig.

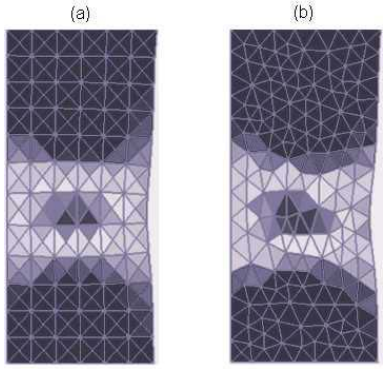

Figure 5: Bias (a) and unbiased mesh (b) with l=3.5 cm in tension test

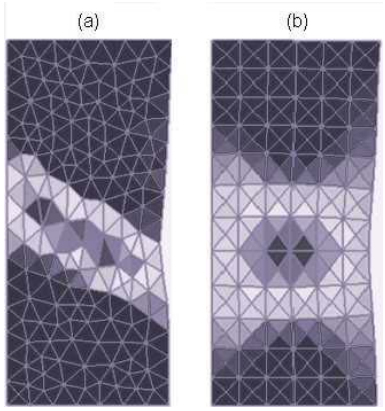

Figure 6: Unbiased meshes with l=2.5 cm (a) and l=5.0 cm (b), in tension test.

6-(a) and (b), respectively.

The numerical analysis in this section with the gradient plasticity model and FE approach in this paper have demonstrated the robustness of the proposed algorithms. In this sense, a super linear convergence rate was obtained, that is consistent with the fixed point iterative procedure considered in the dual mixed FE method.

The numerical tools shown stability during the entire non-lineal process including the formation of the localized failure zone.

The results in this work also demonstrate the capability of non-local gradient-based constitutive formulations in conjunction with the dual mixed FE-approach to regularized the post-peak response behavior of the smeared-crack approach.

IV. CONCLUSIONS

A FE procedure for thermodynamically consistent gradient-dependent plasticity was proposed for CST elements. The procedure consider two uncoupled but sequenced iterative processes for the update of the displacement field and plastic multiplier.

The results in this work demonstrate the efficiency and potentials of the so called *dual mixed method* for

FE analysis of gradient-dependent plasticity. The results further show the strong control of the width of the localization zone by the characteristic length l that characterizes the gradient-based plasticity models.

V. ACKNOWLEDGMENTS

The authors acknowledge the financial support for this work by FONCYT (Argentina Agency for the promotion of research and technology) through the Grant PICT 12/9870 and by FUDETEC (Foundation for Technology Advancement). The second author acknowledge the partial financial support to this work by CONICET (National Council for science and technology) through Grant PIP 3006 and by the University of Tucuman, Argentina, through the Grant 26/E217.

REFERENCES

Etse, G. and K. Willam, "Failure analysis of elasto-viscoplastic material models," *ASCE, Journal of Eng. Mechanics*, **125**, 60-69 (1999).

Hill, R., "Acceleration waves in solids," *J.for Mechanics of Physics and Solids*, **10**, 1-16 (1962).

Nadai, A., *Plasticity*, McGraw, New York (1931).

Ottosen, N. and K. Runesson, "Properties of discontinuous bifurcation in elasto-plasticity," *Int. J. Solids Structures*, **27**, 401-421 (1991).

Perič, D., *Localized deformation and failure analysis of pressure sensitive granular materials,* Ph.D. thesis, University of Colorado, CEAE Dept., Boulder, USA (1990).

Rizzi, E., I. Carol and K. Willam, "Conditions for the localization of deformation in pressure-sensitive dilatant materials," *J. for Mechanics of Physics and Solids*, **121(4)**, 541-554 (1995).

Rudnicki, J. and J. Rice, "Localization analysis of elastic degradation with application to scalar damage," *ASCE, J. Eng. Mech.*, **23**, 371-394 (1975).

Sluys, L., *Wave propagation, localization and dispersion in softening solids,* Ph.D.Thesis, University of Technology, Delft, The Netherlands (1992).

Sobh, N., *Bifurcation analysis of tangential material operators,* Ph.D. thesis, University of Colorado, CEAE Dept., Boulder, USA (1987).

Svedberg, T., *On the Modelling and Numerics of Gradient-Regularized Plasticity Coupled to Damage,* Ph.D.Thesis, Chalmers University of Technology, Sweden (1999).

Thomas, T., *Plastic flow and fracture in solids*, Academic Press, London (1961).

Vrech, S. and G. Etse, "Geometrical localization analysis of gradient-dependent parabolic Drucker-Prager elastoplasticity." In press: *International Journal of Plasticity*, (2005).

Willam, K. and G. Etse, "Failure assement of the extended leon model for plain concrete," *SCI-C* (1990).

Received: August 7, 2005.
Accepted for publication: August 7, 2006.
Recommended by Editor E. Dvorkin.